Depth profiling of dopants in thin gate oxides in complementary metal–oxide–semiconductor structures by resonance ionization mass spectrometry

S. W. Downey, A. B. Emerson, G. E. Georgiou, J. Bevk, R. C. Kistler, N. Moriya, D. C. Jacobson, and M. L. Wise
AT&T Bell Laboratories, 600 Mountain Ave, Murray Hill, New Jersey 07974

The thickness of gate dielectrics for complementary metal–oxide–semiconductor (CMOS) devices with 0.1 to 0.35 μm gate dimensions is typically 4 to 7 nm. Besides serving as an insulator, the dielectric, usually SiO_2, also acts as a diffusion barrier between the doped polycrystalline silicon gate material and the Si substrate (channel). Dopant diffusion from the poly-gate into the device channel may cause undesirable shifts in the transistor threshold voltage. The determination of dopant diffusion through the gate dielectric into the channel region of the transistor is necessary to optimized device processing. This paper reports a method, resonance ionization mass spectrometry (RIMS), to measure dopant distribution profiles near the gate oxide. The pertinent spectroscopy of sputtered B and P atoms is demonstrated. Matrix effects are shown to be diminished. RIMS depth profiles of CMOS test structures show both dopant penetration into the channel and blockage by the gate oxide depending upon annealing conditions. © *1995 American Vacuum Society.*

I. INTRODUCTION

Deep submicron complementary metal–oxide–semiconductor (CMOS) devices with 0.1–0.35 μm gate dimensions require ultra thin gate dielectrics; 4–7 nm equivalent of silicon dioxide thickness. The gate dielectric, besides serving as an insulator, should also act as a diffusion barrier between the doped polycrystalline silicon gate material and the Si substrate (channel). For ultrathin oxides, dopants from the p^+ poly-gate can easily diffuse into the device channel and cause undesirable shifts in the transistor threshold voltage. The determination of dopant diffusion through the gate dielectric into the channel region of the transistor is an important event that needs to be monitored and accurately measured. This paper reports a method to measure dopant distribution profiles at the gate oxide interface for monitoring the dopant diffusion problem.

The tracking of dopant diffusion through layers of materials is difficult by conventional depth profiling techniques. Secondary ion mass spectrometry (SIMS) has the sensitivity required to detect dopants at the part-per-million (ppm) level or below, but is hindered by its matrix dependent ionization yield (matrix effect). This is especially true when the layer thickness is of the order of the depth resolution of the instrument, as in the CMOS gate oxide case. A steady-state matrix composition may not be reached because the length scale of sputter-induced mixing of material may be comparable to the layer thickness. The secondary ion yield may never reach an equilibrium value, thus precluding the accurate use of relative sensitivity factors for a given material. The gate oxide structure in CMOS is particularly difficult to profile through with accuracy because oxides exhibit high secondary ion yields relative to other materials. Therefore tracking dopant diffusion at, near or through the thin gate oxide is particularly ambiguous by SIMS.

In CMOS gate structures, the information desired is usually the amount of dopant from the polysilicon that diffuses through the gate oxide into the channel region. See Fig. 1. The polysilicon contains high dopant (B, P, or As) concentration ($>10^{19}$ cm^{-3}) for good conductivity, and is only 10 nm or less (the gate oxide thickness) from the channel where the dopant's intended concentration may be $<10^{16}$ cm^{-3}, depending on device design. Stated another way, a sub-part-per-million measurement is being performed less than 10 nm from material that contains part-per-thousand analyte. Excellent spatial (depth) resolution and detection sensitivity are therefore necessary to attempt this measurement. The polysilicon may not sputter as smoothly as single crystal Si, possibly degrading the depth resolution in the gate oxide region. High dynamic range measurements are necessary because the total dopant's concentration in the polysilicon needs to be determined and compared with the measured amount of electrically active dopant in the polysilicon.

Post-ionization of sputtered neutral atoms or molecules is one proven method of alleviating the problematic matrix effects associated with depth profiling of layered Si based materials.[1] As the different layers are removed by ion beam sputtering, the flux of detected neutral particles, (atoms) changes only by an amount proportional to the change in relative sputtering rates. In the case of SiO_2 and Si, the change in relative sputter rates is only about 10%. By contrast, the change in relative secondary ion yield is nearly a factor of ten.[2] Post-ionization of gas-phase atoms with tunable laser radiation, so called "resonance ionization" coupled with mass spectrometry (RIMS), possesses the sensitivity to detect low levels of B and P atoms sputtered from CMOS test structures. Moreover, matrix effects are minimized in the mulitilayer test structures. Accurate profiles of dopant diffusion are possible, thus assisting in materials characterization and in determining optimum process parameters for device fabrication.
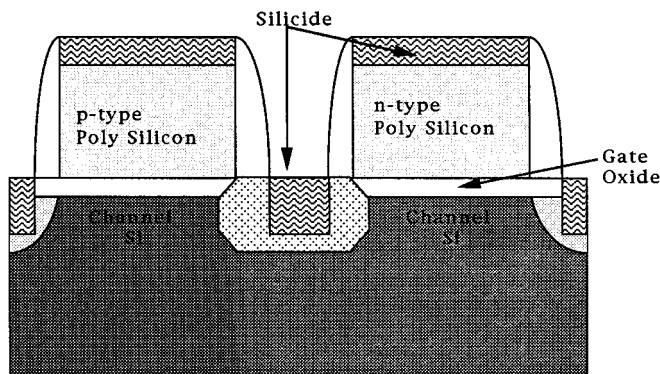
FIG. 1. Schematic diagram of channel regions of CMOS transistors (not to scale). CMOS is composed of *p*-type MOS (PMOS) (left) and *n*-type MOS (NMOS) (right) on same chip. For depth profiling measurements, the samples are composed of planar Si, gate oxide, polysilicon with or without silicide, and contain one dopant.

II. EXPERIMENT

The RIMS instrument, previously described,[1] has several noteworthy modifications to meet the high dynamic range and sensitivity requirements of CMOS dopant profiling. The dopant concentration may change by five orders of magnitude (or more) during a depth profile, which means the RIMS signal arises from about 100 to 0.001 ions detected per laser shot. Two detection modes are needed to cover this large range; current measurements when signals are greater than about one ion per laser shot, and ion integration when count rates are slightly less than one per shot. Analog detection is performed by averaging the output of a Daly detector with a gated integrator. Digital pulse counting is performed by a time gated counter monitoring the output of an electron multiplier biased for ion detection. Both time gates are 3 μs wide, and are synchronized to the laser's firing and delayed by the ions' flight time to the detectors. During the depth profile, the gain of the Daly detector may be varied by software control in order to keep signals on scale. High and low set points on the measured signal are used to increase or decrease the detector gain and switch to pulse counting when necessary. Pulse counting is required when the dopant concentration is about 1 to 10 ppm when sputtering with 1 μA of beam current. A Xe^{+} primary ion beam, produced by a mass filtered duoplasmatron source, is used for sputtering to keep the neutral atom yield high.

Data are obtained in alternating continuous and pulsed sputtering modes. In this way, the amount of material removed between data points and the integration times are independently selected. Rastering of the ion beam creates a flat bottomed crater for the analysis cycle. Typical sputtering times are 1–2 s, during which about 1 nm of material is removed. The crater bottom is examined under static (pulsed) sputtering conditions for both analog and pulse counting detection. The laser is timed to fire when the beam is in the crater's center, thus avoiding edge contamination where the dopant concentration may be high. The beam's potential is between 2 and 6 kV relative to the sample. At the lowest voltage, large craters are formed[1] which also helps reduce crater edge effects. At 6 kV, the beam's angle of

incidence is about 30° from the surface normal, while at 2 kV, the angle is approximately 60°.

Because mass switching and long integration times are required to detect sputtered atoms at low concentrations, an improved, high-speed voltage (<25 ns rise and fall time, 0 to 1.5 kV) pulser is used for primary ion beam blanking. Sub microsecond ion pulses provide sufficient atomization for the photoionization process while conserving sample. In these experiments, 600 ns sputtering pulses (at 40 Hz) are used to keep the primary ion beam's dose rate during data acquisition cycles below 10^{12} ions/cm^2 s. Typically, 0.4–1.0 μA are contained in a 100 μm diameter beam. Integration times of several minutes are therefore possible before the effective dose required to remove one monolayer of Si is delivered to the sample. In that time, the ions from several thousand laser shots may be collected, the mass spectrometer scanned, and a matrix ion, ^{28}Si or ^{44}(SiO), monitored with the analog detector for interfacial marking.

In this work, ^{11}B and ^{31}P atoms are ionized by laser light with wavelengths of approximately 250 and 300 nm, respectively, produced by frequency doubling of an excimer-pumped dye laser. Two separate dye circulation systems are used to obtain the fundamental wavelengths for doubling, one for Coumarin dyes (green) and one for Rhodamine dyes (red). Inter-dye contamination is avoided and relatively rapid conversion between wavelengths is possible. The optical system that transports the light to the vacuum chamber is comprised of either mirrors or prisms. The former gives slightly greater reflectivity while the latter is suitable for both wavelength regions.

Two types of samples with test structures based on the 0.25 and 0.35 μm symmetric CMOS technologies are investigated. For illustrative, comparitive, and calibration purposes, a boron implanted (26 keV, 1×10^{15} cm^{-2}) Si/SiO$_2$ test structure is also examined. The SiO$_2$ layer is 100 nm in this structure and the implant is designed to put about one half the boron in each material. This sample was profiled before and after the SiO$_2$ layer was removed by HF solution etching. In this way, the effect of the oxide on SIMS and RIMS signals are easily compared. The dose was independently calibrated by the ^{11}B$[p,\alpha]$ nuclear reaction analytical technique[3] on the stripped sample, verifying that the amount of B in the substrate Si is 4.95×10^{14} cm^{-2}.

One set of CMOS samples has 200 nm of polysilicon on 6.3 nm of SiO$_2$ on Si and is implanted with B (5 keV, 5×10^{15} cm^{-2}) followed by rapid thermal annealing (RTA) at 1050 °C for 10 s and by 850 °C annealing for 1 or 2 hours. Prior to oxide growth, the wafers are cleaned by etching in 100:1 HF:water for 2 min. The oxide is then grown in dry O$_2$ at 800 °C. The thickness is determined by ellipsometry prior to polysilicon deposition. The polysilicon is grown at 550 °C with SiH$_4$ based chemical vapor deposition (CVD). One piece of this wafer was not implanted or annealed to check for nascent B contamination.

The second set of CMOS samples is implanted with P or BF$_2$ (5×10^{15} cm^{-2}). These samples are similar to that depicted in Fig. 1 and have 100 nm of WSi$_{2.5}$ on 100 nm of polysilicon on 9 nm of SiO$_2$ on Si. This structure is fabricated similarly, the gate oxide grown at 850 °C immediately
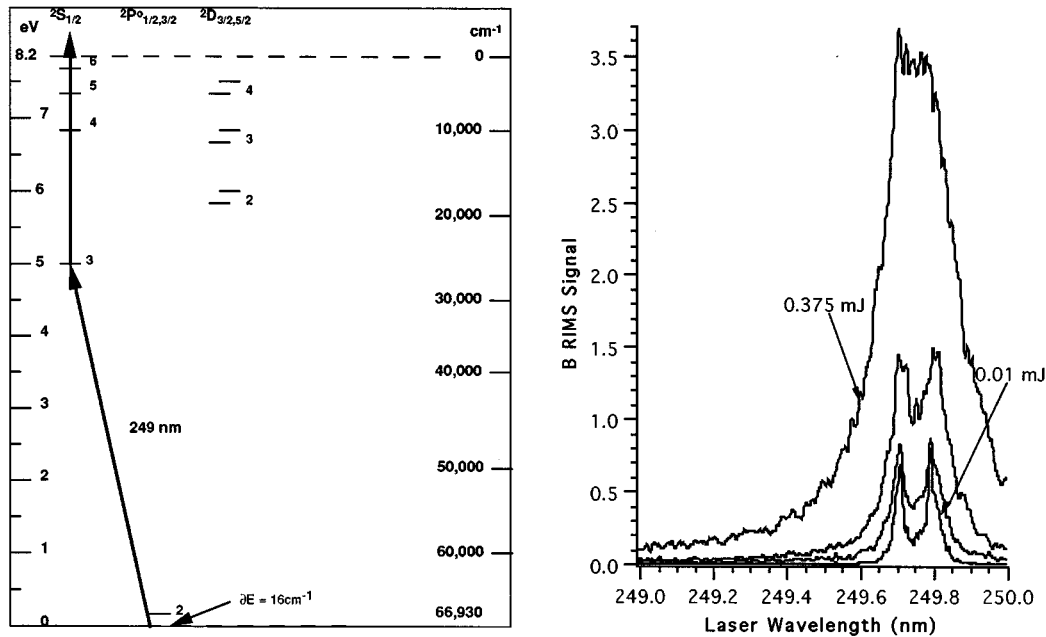
FIG. 2. Partial electronic energy levels of atomic B (left) and RIMS signal at various laser pulse energies showing the broadening of the ground state doublet at higher powers (right). The traces without labels correspond to the intermediate energies of 0.087 and 0.20 mJ.

followed by the deposition of 100 nm polysilicon at 600 °C. Sputter deposition of 100 nm $WSi_{2.5}$ is followed by the liquid phase CVD (LPCVD) deposition of 100 nm SiO_2. P (100 keV) or BF_2 (110 keV) is implanted and then diffused with a 1050 °C, 10 s and 850 °C 30 min anneal cycle. The 100 nm is SiO_2 is stripped prior to analysis.

The resonance ionization of B atoms is achieved with two photons at 249.7 nm. See Fig. 2. This "1+1" process, one resonance photon plus one ionization photon, is slightly complicated by the spin-orbit splitting of the $^2P^0_{(J=1/2,3/2)}$ ground state. The two components are separated in energy by a small amount, 16 cm^{-1} (about 2 meV) and should be equally populated by the energetics of sputtering. The statistical population $(2J+1)$ ratio of $^2P^0_{3/2}:^2P^0_{1/2}$ should be 4:2. No other low lying states in B exist. Figure 2 shows that at low power, the signal out of the higher energy (longer wavelength transition) state, $J=3/2$, has slightly more integrated intensity. To obtain the greatest RIMS signals however, both states must simultaneously be addressed by the laser. This is achieved in this single laser system by increasing the pulse energy sufficiently to broaden the two lines of the spectral doublet together. The line widths grow proportionally to $I^{1/2}$, where I is the laser intensity. Fortunately, the ground state splitting in B is small enough that the ionization from both levels can be saturated (100%) with 1 mJ or more of energy (about 10^7 W/cm^2). Other group III elements, like Al, have larger splittings precluding the simultaneous ionization of both components of the ground state.[4] Remaining above the threshold for saturation intensity is desirable to ensure that the sensitivity for B does not change as the laser's output gradually decreases during a depth profile. Saturation is also necessary for quantitative B measurements.[5] After each B depth profile is obtained, the laser pulse energy is measured

to ensure that the detection sensitivity has not changed.

The resonance ionization of P atoms (Fig. 3) is more complicated than B because the ionization potential of P is high (11 eV). However, the ground state splitting is large for the $3p^3$ electrons, the $^2D^0$ and $^2P^0$ states are greater than 1 and 2 eV, respectively, above the $^4S^0$ lowest energy state. Nearly all the sputtered atomic P will be in the $^4S^0$ level and available for resonance ionization by a single wavelength. The simplest 1+1 ionization process for P would require 178 nm laser light, which is very difficult to produce and transport through air. P can be ionized with three photons at 299.2 nm by a simultaneous two photon resonance plus an ionization photon $(2+1)$.[6] High intensity is required to saturate the resonance and ionization steps, about 10^8 W/cm^2, which is difficult to achieve and maintain with the present laser system. In addition, a tighter focus of the laser beam may be required to reach high intensity which reduces the volume of atoms probed. Therefore the detection limit is reduced somewhat relative to B. The count rate for P is roughly about one fifth of that for B of comparable concentration. High intensity ultraviolet light may ionize sputtered $^{30}Si^1H$, which has the same nominal mass as ^{31}P. Initial results suggest this interference will be significant when making P determinations below 1 ppm.

III. RESULTS AND DISCUSSION

Prior to investigating B diffusion in CMOS thin gate oxides, RIMS and SIMS are evaluated in the Si/SiO$_2$ materials system. A boron implanted test structure consisting of 100 nm of SiO$_2$ on Si is used to compare the change in relative sensitivities for B during depth profiling across the Si/SiO$_2$ interface. Xe$^+$ sputtered RIMS profiles are compared with
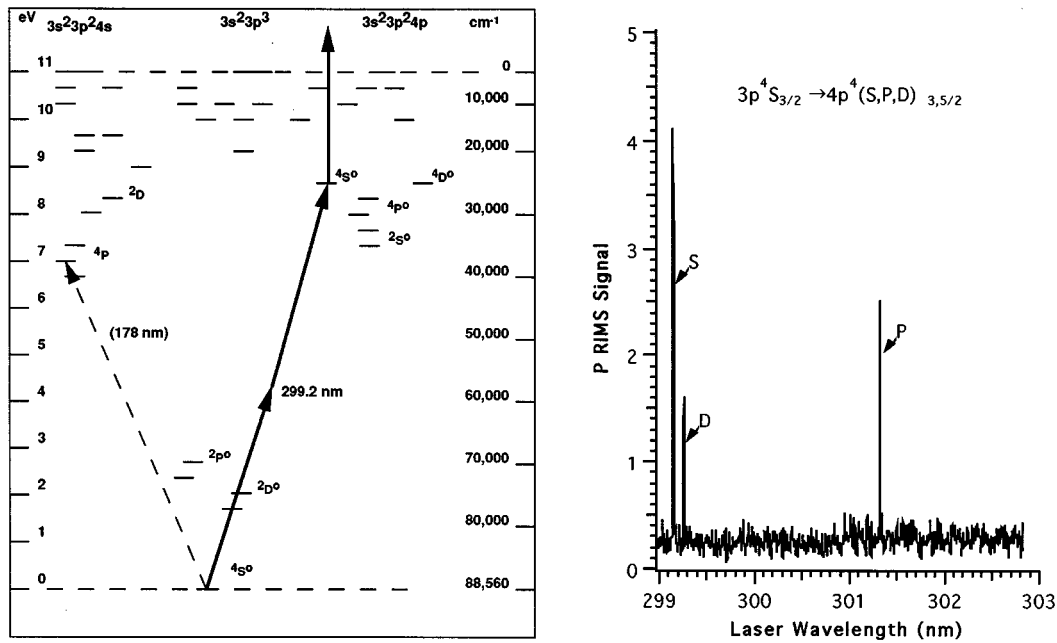
FIG. 3. Partial electronic energy levels of atomic P (left) and RIMS spectrum (right). The upper state designation is given in the spectrum. All transitions originate in the $^4S°$ ground state. The peaks are narrow due to the simultaneous two photon resonance.

coventional O_2^+ sputtered SIMS profiles. Xenon enhances the sputtered atom yield. Figure 4 shows a pronounced change in relative sensitivity in the B SIMS profile at the Si/SiO$_2$ interface. The yield enhancement here for B is eight to nine times greater in SiO$_2$ relative to Si with O_2^+ sputtering, consistent with reported values.[2] The change in SIMS yield for B with Xe$^+$ sputtering is about a factor of 100. Correction of matrix effects by SIMS relative sensitivity factors[2] (RSF) is possible when a steady-state change in materials is achieved. However, the width of the SiO$_2$ is comparable to the mixing width of the ion beam in the case of the thin gate oxide. The sputtered sample never reaches a constant composition where one RSF is applicable. Procedures have been devised to correct for sputter rate and ion yield changes across a single interface,[17] but they make many assumptions, including linear compositional change across the sputtered interface[8] and ideal instrument performance. By contrast, the RIMS profile through the oxide shows no significant change in relative sensitivity for B between the two materials. The results from the sample with the SiO$_2$ layer stripped by HF etching prior to analysis confirm that both techniques give identical profiles in the absence of a changing matrix.

The ability of RIMS to suppress matrix effects in the thin gate oxide region of a CMOS structure is shown in Fig. 5. For comparison, the SIMS profile shows a pronounced peak in the B profile in the SiO$_2$, which is expected even if no B exists in this layer, due to sputter-induced mixing of the B containing polysilicon and the yield enhancing oxygen from the SiO$_2$. The increase here in B SIMS counts is only a factor of three, consistent with the true B concentration being lower in the oxide than in the polysilicon but complicated by the higher yield for B ions in the SiO$_2$. As sputtering proceeds into the channel region below the gate oxide, the B

secondary ion yield changes again (decreases).

By contrast, the RIMS profile in Fig. 5 shows no B spike at the polysilicon/gate oxide interface, eliminating the interpretation of a B pile-up at this location. Although the layers are mixed by sputtering, there is no drastic change in sputtered atom yield (no matrix effect) as the layers are removed. No correction for relative sensitivity changes are required. Both RIMS and SIMS profiles show degraded depth resolution, due to roughening while sputtering through 200 nm of polycrystalline material prior to reaching the gate oxide. In
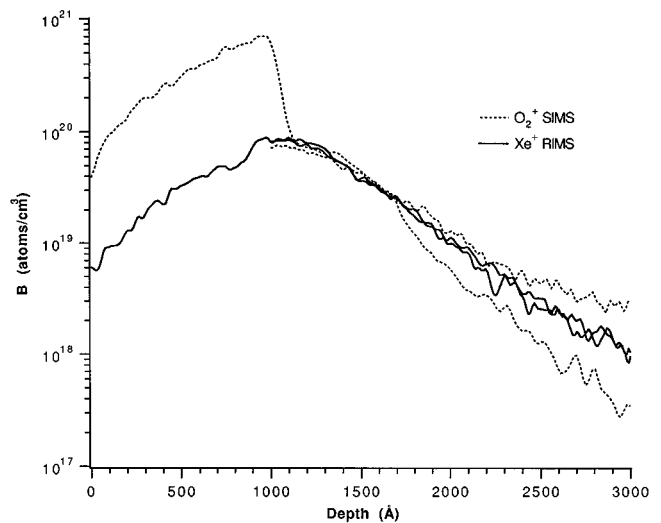

FIG. 4. SIMS and RIMS B depth profiles of B implanted (26 keV, $1×10^{15}$ cm^{-2}) sample consisting of 1000 Å SiO$_2$ on Si. The sample is sputtered with 4 keV primary ions. The two profiles that start at 1000 Å are from a portion of the sample that was stripped of the SiO$_2$ prior to profiling using aqueous HF.
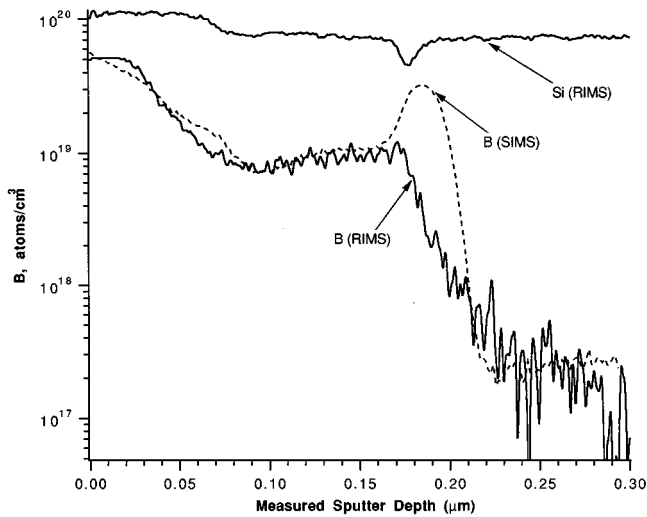
FIG. 5. SIMS and RIMS B depth profiles of a test CMOS structure. The layers are from top: 100 nm WSi$_2$ on 100 nm polysilicon on 9 nm gate oxide on Si. The sample is implanted with 25 keV BF$_2$ (5×10^{15} cm^{-2}) followed by rapid thermal annealing 1050 °C, 10 s, and 850 °C annealing for 0.5 h. The sample is sputtered with 6 keV primary ions: SIMS—O$_2^+$, RIMS—Xe$^+$. Only analog detection was used in the RIMS profiles. The Si RIMS signal is arbitrarily scaled and shows the location of the gate oxide (dip).
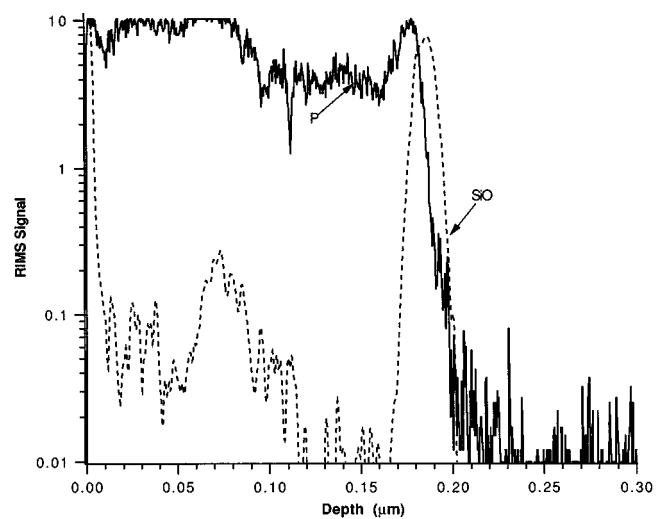
FIG. 6. RIMS depth profile of test P implanted CMOS structure. The sample and implant parameters are the same as for the B sample in Fig. 5. The sample is sputtered with 6 keV Xe$^+$ primary ions. Only analog detection is used, and the P signal is just off scale around 0.075 μm. ^{44}(SiO) is used to mark the gate oxide.

addition, the 6 keV ions used to sputter exacerbates the layer mixing somewhat. Superior depth resolution is demonstrated later. The SIMS profile appears to have a sharper transition on the trailing edge of the B profile, but this is in part because of the decrease in secondary ion yield as the sputtering progresses into the channel Si as explained above.

In Fig. 5, the change in Si RIMS signal was used to delineate the thin gate oxide layer. From previous measurements,[1] it is known that the Si RIMS signal from Si and SiO$_2$ changes in proportion to the Si concentration. The dip in the Si signal at the gate oxide changes by not quite a factor of two and has a full width at half maximum (FWHM) of 10 nm, indicative of some deterioration of depth resolution due to sputtering through the polycrystalline material. Note that the Si signal in the polysilicon and bulk Si is the same, indicating no difference in sputter rates in the two materials. Also seen is the decrease in Si signal as sputtering proceeds from the WSi$_2$ layer into the polysilicon. Although the atomic density (atoms/cm^3) of Si is 8% greater in Si than in WSi$_2$, the Si RIMS signal is greater from WSi$_2$ than Si. In the absence of large sputtered molecular fractions,[9] changes in RIMS signals are proportional to sputter rate changes between materials. To explain the data, the WSi$_2$ sputter rate must be 1.3 that of Si. This sputter rate ratio is evident in the location of the WSi$_2$/ polysilicon interface on the linear depth scale, which is not corrected for such changes. The 100 nm WSi$_2$ layer (confirmed by RBS and profilometry of a crater terminated at the WSi$_2$/ polysilicon interface) is depicted as being about 70 nm thick. WSi$_2$ sputters faster (greater sputter yield) due to the large W atoms having a more efficient energy and momentum transfer with the incoming Xe$^+$. By comparison, sputter rates for silicides with O$_2^+$ bombardment are typically less than that for Si.[2,8] In Fig. 5, the B SIMS profile may be shifted slightly relative to the gate oxide due

to the small sputter rate change or the accuracy of the profilometry of the two craters. This phenomenon, based on sputter rate difference is prevalent in SIMS and RIMS.

Figure 6 shows an example where RIMS detects the dopant pile-up at the polysilicon/gate oxide interface. In this case, P diffusion appears to be stopped by the gate oxide. SIMS of this sample is not performed for comparison because negative ion detection and Cs$^+$ sputtering are not possible here, but profiles obtained on other instruments show an increased P$^+$ yield at the interface similar to the B SIMS data in Fig. 5. Their interpretation is also ambiguous because of the matrix effect. In this sample, the RIMS signal from the sputtered SiO molecule was used as an interface marker. This species is detected with unknown efficiency at the P resonance wavelength, 299.2 nm, but is traceable in sufficient concentration to delineate the gate oxide layer. The broad SiO feature near 0.07 to 0.08 μm also shows evidence of an irregular interface and the oxidation of the rough polysilicon surface during sample fabrication prior to the WSi$_2$ deposition. The P RIMS signal is also very noisy, in part due to the roughened surface.

Surface and interfacial B contamination can be detected with good reliability using RIMS. Figure 7 show the B and SiO profiles of a CMOS test structure prior to ion implantation. Boron is detected at the polysilicon/gate oxide interface and on the surface. The surface contamination of this and similar samples is between 10 and 100 parts per million (10 ppm$\approx10^{10}$ cm^{-2}), which is slightly less than results from other work on Si surface contamination with B.[10] As in Fig. 6, the SiO species is used to mark the gate oxide layer because sufficient ionization occurs at 249.7 nm. This wavelength is near that for the strongly allowed $X\rightarrow A$ $^1\Sigma^+ - ^1\Pi$ transition in SiO.[11] Because of the absence of significant matrix effects, the B peak at the gate oxide layer is noticed to be slightly forward from the peak in the
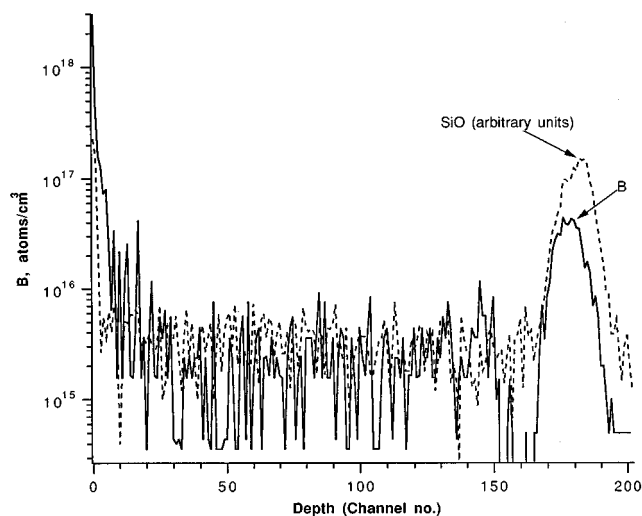
FIG. 7. Depth profile of test CMOS structure prior to B implantation. The sample is 200 nm of polysilicon on 6.3 nm of SiO_2 on Si. The B contamination is at the polysilicon/gate oxide interface. The profile was obtained with 2 keV Xe^+ sputtering. The $^{44}(SiO)$ intensity is arbitrary. The integrated B concentration at the polysilicon/gate oxide interface is about 2×10^{10} cm^{-2}.

SiO signal. This indicates that the B is at the polysilicon interface and not the channel Si interface. This result is not too surprising, but is exemplary of the interfacial sensitivity of RIMS. Importantly, the residual B contamination, the result of normal handling and processing, is not in the channel Si but at the polysilicon/gate oxide interface.

Figure 8 shows how the effect of different CMOS processing steps can be monitored by RIMS. Pieces of the same wafer were subjected to different annealing conditions to examine potentially deleterious B diffusion. Samples with RTA only or RTA plus additional annealing are examined. The sample with RTA only exhibits what appears to be minimal B migration into the SiO_2. However, it is unclear whether the slight difference in B profiles is due to B diffusion or to a modification of the material (mainly polysilicon crystallinity) during annealing which affects the sputter-induced broadening of the profiles.

This type of sample analysis pushes the limits of depth resolution of any sputtering-based depth profiling technique. In fact, the definition of depth resolution needs to be examined. A useful parameter to describe the depth resolution is the decay length (nm of measured sputter depth per decade signal decrease) of an abrupt layer. In the absence of diffusion, the B containing polysilicon layer approximates this condition. If depth profiles are obtained under ideally identical conditions, then differences in B decay length may be used to discuss relative differences in B profiles between samples. In the sample with RTA only, the B decay length is 5.5 nm; for the one hour annealed sample, it is 8.0 nm. The depth scales, and hence decay lengths were determined in two ways: (1) A profilometer measurement of the sputtered crater and (2) assignment of the peak of the SiO signal to be 0.2032 μm, the center of the gate oxide. The methods of assigning depth agree to within 5%, comparable to the precision of the profilometer and layer thickness control.
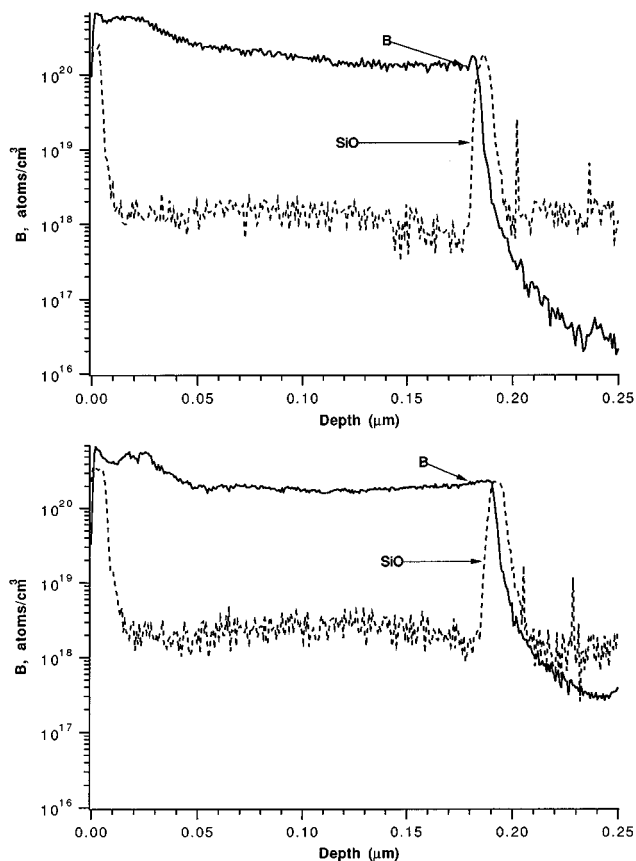

FIG. 8. Depth profiles of B implanted (5 keV B^+, 5×10^{15} cm^{-2}) test CMOS structures as described in Fig. 7. Following implantation, the samples were heated by rapid thermal annealing at 1030 °C for 10 s (top), then annealed at 800 °C for 1 h (bottom). The $^{44}(SiO)$ peak is also profiled, locating the gate oxide.

It is well known that lower energy primary ions[12] at higher angle of incidence[13] optimize depth resolution (small decay lengths) by keeping the penetration depth of the incident ions low. In this work, 2 keV Xe^+ sputtering at high angle of incidence is used to minimize the broadening of the profiles. Although not directly comparable, these decay lengths are in reasonable agreement with those given previously for Xe^+ sputtering at 60° incidence and 12 keV in

TABLE I. The results of RIMS depth profiles of B implanted (5 keV B^+, 5×10^{15} cm^{-2}) test CMOS structures. These samples consist of 0.2 μm of polysilicon on 6.2 nm of gate oxide on Si. Following implantation, all samples were heated by rapid thermal annealing at 1030 °C for 10 s. Some samples then had furnace annealing. The $^{44}(SiO)$ peak is also profiled to check the depth resolution. The decay length refers to how rapidly the B signal is decreasing through the gate oxide.

Anealing conditions	Gate oxide FWHM (nm)	Decay length (nm/decade)	[B] in channel Si (atoms/cm^3)
RTA only	7.7	5.0	2×10^{16}
800 °C, 1 h	7.5	5.9	3×10^{17}
850 °C, 1 h	7.0	7.5	2×10^{17}
900 °C, 1 h	7.0	5.0	1×10^{17}
850 °C, 2 h	8.0	8.3	2.5×10^{17}

B-doped polysilicon,[13] and for 2 keV at 2° incidence in deposited Si.[12]

The total B concentration in the polysilicon films is the same, 5×10^{15} cm^{-2} as confirmed by the ^{11}B$[p,\alpha]$ nuclear reaction analytical technique[3] and consistent with the known implanted B dose. The average concentration in the 200 nm thick polysilicon film is 2.5×10^{20} cm^{-3}. The practical absence of matrix effects allows relative signals to be used to estimate the B diffused into the Si. The B signal from the RTA only sample decays by more than 4 orders of magnitude, to about 2×10^{16} cm^{-3} in the substrate Si, while the samples with further annealing decays only 3 orders of magnitude, to about 3×10^{17} cm^{-3}. This latter level is significantly higher than the typical B background in the instrument, so with good confidence it can be concluded that B significant diffusion through the thin gate oxide has occurred. See Table I for a summary of B diffusion into the channel Si as a function of additional annealing. The ^{44}(SiO) peak widths exhibit no obvious systematic trends with decay length, indicating the depth resolution is approximately constant in all the samples profiled.

IV. CONCLUSIONS

Resonance ionization mass spectrometry has been further developed to measure B and P depth profiles in CMOS materials. The determination of these dopants at or near interfaces in layered devices is simplified by the absence of significant matrix effects. Small yet significant differences in dopant distributions created by changing processing parameters may be detected.

[1]S. W. Downey and A. B. Emerson, Surf. Interface Anal. **20**, 53 (1992).
[2]R. G. Wilson, F. A. Stevie, and C. W. Magee, *Secondary Ion Mass Spectrometry: A Practical Handbook for Depth Profiling and Bulk Impurity Analysis* (Wiley, New York, 1989).
[3]L. C. Feldman and J. W. Mayer, *Fundamentals of Surface and Thin Film Analysis* (North-Holland, New York, 1986).
[4]S. W. Downey, A. B. Emerson, and R. F. Kopf, J. Vac. Sci. Technol. B **10**, 385 (1992).
[5]S. W. Downey and A. B. Emerson, Anal. Chem. **63**, 916 (1991).
[6]O. Gobert, B. Dubreuil, R. L. Inglebert, P. Gelin, and J. L. Debrun, Phys. Rev. A **41**, 6225 (1990).
[7]D. S. McPhail and S. D. Littlewood, in *Secondary Ion Mass Spectrometry, SIMS VIII*, edited by A. Benninghoven, C. A. Evans, A. M. Huber, K. D. McKeegan, H. A. Storms, and H. W. Werner (Wiley, New York, 1992), p. 407.
[8]S. F. Corcoran, C. M. Osburn, N. Parikh, R. W. Linton, and D. P. Griffis, J. Vac. Sci. Technol. A **7**, 3065 (1989).
[9] S. W. Downey, A. B. Emerson, and R. F. Kopf, Nucl. Instrum. Methods Phys. B **62**, 456 (1992).
[10]F. A. Stevie, E. P. Martin, P. M. Kahora, J. T. Cargo, A. K. Nanda, A. S. Harrus, A. J. Muller, and H. W. Krautter, J. Vac. Sci. Technol. A **9**, 2813 (1991).
[11]K. P. Huber and G. Herzberg, *Molecular Spectra and Molecular Structure* (Van Nostrand, New York, 1979).
[12]K. Wittmaack and D. B. Poker, Nucl. Instrum. Methods. Phys. Res. B **47**, 224 (1990).
[13]R. v. Criegern and I. Weitzel, in *Secondary Ion Mass Spectrometry SIMS V*, edited by A. Benninghoven, R. J. Colton, D. S. Simons, and H. W. Werner (Springer, Berlin, 1986), p. 319.